



Published in final edited form as:

Circulation. 2020 April 21; 141(16): 1318–1333. doi:10.1161/CIRCULATIONAHA.119.043385.

Local Peroxynitrite Impairs Endothelial TRPV4 Channels and Elevates Blood Pressure in Obesity

Matteo Ottolini, M.S.^{†,1,2}, Kwangseok Hong, Ph.D.^{†,1}, Eric L. Cope, B.S.¹, Zdravka Daneva, Ph.D.¹, Leon J. DeLalio, Ph.D.¹, Jennifer D. Sokolowski, M.D. Ph.D.³, Corina Marziano, Ph.D.^{1,4}, Nhiem Y. Nguyen, B.S.¹, Joachim Altschmied, Ph.D.⁵, Judith Haendeler, Ph.D.^{5,6}, Scott R. Johnstone, Ph.D.¹, Mohammad Y. Kalani, M.D. Ph.D.³, Min S. Park, M.D.³, Rakesh P. Patel, Ph.D.⁷, Wolfgang Liedtke, M.D., Ph.D.⁸, Brant E. Isakson, Ph.D.^{1,4}, Swapnil K. Sonkusare, Ph.D.^{1,2,4,*}

¹Robert M. Berne Cardiovascular Research Center, University of Virginia-School of Medicine, Charlottesville, VA, 22908, USA

²Department of Pharmacology, University of Virginia-School of Medicine, Charlottesville, VA, 22908, USA

³Department of Neurological Surgery, University of Virginia, Charlottesville, VA, 22908, USA

⁴Department of Molecular Physiology and Biological Physics, University of Virginia-School of Medicine, Charlottesville, VA, 22908, USA

⁵IUF-Leibniz Research Institute for Environmental Medicine, Duesseldorf, 40021, Germany

⁶Institute of Clinical Chemistry and Laboratory Diagnostic, Medical Faculty, University of Duesseldorf, Duesseldorf, 40021, Germany

⁷Department of Pathology and Center for Free Radical Biology, University of Alabama at Birmingham, Birmingham, AL, 35294, USA

⁸Department of Neurology, Duke University School of Medicine, Durham, NC, 27710, USA

Abstract

Background—Impaired endothelium-dependent vasodilation is a hallmark of obesity-induced hypertension. The recognition that Ca²⁺ signaling in endothelial cells promotes vasodilation has led to the hypothesis that endothelial Ca²⁺ signaling is compromised during obesity, but the underlying abnormality is unknown. In this regard, TRPV4 ion channels are a major Ca²⁺ infl

*Correspondence should be addressed to: Swapnil K. Sonkusare, Ph.D., Room 6051A, Medical Research Building 4 (MR4), 409 Lane Rd, University of Virginia-School of Medicine, Charlottesville VA 22908, sks2n@virginia.edu, Phone: 434-297-7401.

[†]Authors contributed equally

Author Contributions. SKS conceptualized the study and obtained funding. SKS, MO, and KH designed the experiments. SKS and MO wrote the manuscript. MO, KH, SKS performed Ca²⁺ imaging and immunostaining. MO performed patch clamp and PLA. ELC and ZD performed diameter experiments. MO, ELC, and NN performed qPCR and genotyping. SRJ, CM, JA, and JH generated the plasmids. ZD, LJD, and BEI conducted blood pressure measurements. RPP helped with redox experiments. WL provided TRPV4^{flox/flox} mice.

Conflict of Interest Disclosures.

None.

pathway in endothelial cells, and regulatory protein AKAP150 enhances the activity of TRPV4 channels.

Methods—We used endothelium-specific knockout mice and high fat diet-fed mice to assess the role of endothelial AKAP150-TRPV4 signaling in blood pressure regulation under normal and obese conditions. We further determined the role of peroxynitrite, an oxidant molecule generated from the reaction between nitric oxide (NO) and superoxide radicals, in impairing endothelial AKAP150-TRPV4 signaling in obesity, and assessed the effectiveness of peroxynitrite inhibition in rescuing endothelial AKAP150-TRPV4 signaling in obesity. The clinical relevance of our findings was evaluated in arteries from non-obese and obese individuals.

Results—We show that Ca^{2+} influx through TRPV4 channels at myoendothelial projections (MEPs) to smooth muscle cells decreases resting blood pressure in non-obese mice, a response that is diminished in obese mice. Counterintuitively, release of the vasodilator molecule NO attenuated endothelial TRPV4 channel activity and vasodilation in obese animals. Increased activities of iNOS and NOX1 enzymes at MEPs in obese mice generated higher levels of NO and superoxide radicals, resulting in increased local peroxynitrite formation and subsequent oxidation of the regulatory protein AKAP150 at cysteine 36, to impair AKAP150-TRPV4 channel signaling at MEPs. Strategies that lowered peroxynitrite levels prevented cysteine 36 oxidation of AKAP150, and rescued endothelial AKAP150-TRPV4 signaling, vasodilation, and blood pressure in obesity. Importantly, peroxynitrite-dependent impairment of endothelial TRPV4 channel activity and vasodilation was also observed in the arteries from obese patients.

Conclusions—These data suggest that a spatially restricted impairment of endothelial TRPV4 channels contributes to obesity-induced hypertension, and imply that inhibiting peroxynitrite might represent a strategy for normalizing endothelial TRPV4 channel activity, vasodilation, and blood pressure in obesity.

Keywords

Obesity-induced hypertension; endothelial dysfunction; calcium signaling; TRPV4 ion channel; peroxynitrite; nitric oxide signaling

Introduction

According to the World Health Organization, the incidence of obesity worldwide has nearly tripled since 1975, affecting ~650 million adults in 2016. Obesity has become a life-threatening health concern and a major risk factor for cardiovascular disease, including hypertension and stroke^{1, 2}. Loss of endothelium-dependent vasodilation is commonly observed in human patients^{3, 4} and animal models of obesity^{5, 6}, and is thought to be a major contributor to obesity-induced hypertension². Therefore, identifying the molecular mechanisms of obesity-induced endothelial dysfunction may help to realize new strategies for therapeutic intervention that offer the promise of improved global health.

Endothelial cell (EC) Ca^{2+} signaling is a key regulator of vascular function⁷. In small, resistance arteries, spatially localized Ca^{2+} signals cause endothelium-dependent vasodilation and diminished vascular resistance^{8–10}. These Ca^{2+} signals can occur through Ca^{2+} release from the endoplasmic reticulum (ER) and/or Ca^{2+} influx through ion channels

at the EC membrane. Notably, elementary Ca^{2+} -influx signals through endothelial transient receptor potential vanilloid 4 (TRPV4_{EC}) channels localized at EC projections to smooth muscle cells (SMCs), termed myoendothelial projections (MEPs), activate nearby Ca^{2+} -sensitive, intermediate- or small-conductance K^+ (IK and SK, respectively) channels to hyperpolarize the EC plasma membrane⁷. This hyperpolarization is subsequently transmitted to surrounding SMCs via myoendothelial gap junctions (MEGJs) that electrically couple ECs and SMCs^{11, 12}. SMC hyperpolarization, in turn, inactivates voltage-dependent Ca^{2+} channels to attenuate Ca^{2+} influx, resulting in vasodilation. Importantly, TRPV4_{EC} channels exhibit cooperative gating, an effect that is enhanced for channels localized to MEP sites. A-kinase anchoring protein 150 (AKAP150), which anchors protein kinase C (PKC) and protein kinase A (PKA)^{13, 14} and is preferentially localized to MEPs in resistance arteries¹⁵, is a crucial enhancer of TRPV4 channel activity in multiple cell types^{15, 16}. However, whether the endothelial AKAP150 (AKAP150_{EC})-TRPV4_{EC} signaling cascade exerts a tonic influence on resting blood pressure, and how this cascade might operate in obesity, remain unknown.

Resistance arteries control the blood pressure, however, the mechanisms for obesity-induced endothelial dysfunction in resistance arteries remain unknown. In large conduit arteries, obesity is associated with excessive formation in ECs of reactive oxygen species (ROS), including the superoxide radical ($\text{O}_2^{\cdot-}$)^{17, 18}. This abnormality, together with the finding of elevated vascular inducible nitric oxide synthase (iNOS) activity^{19, 20}, may catalyze the reaction of $\text{O}_2^{\cdot-}$ with nitric oxide (NO) to form peroxynitrite (PN)²¹, which has been linked to endothelial dysfunction in conduit arteries^{22, 23}. Thus, the common vasodilator molecule NO may have deleterious effects on vasodilation and blood pressure in obesity via PN formation.

Here, we postulated that PN impairs endothelial AKAP150_{EC}-TRPV4_{EC} signaling at MEPs to curtail endothelium-dependent vasodilation and elevate blood pressure in obesity. Using newly developed endothelium-specific AKAP150 (AKAP150_{EC}^{-/-}) and TRPV4 (TRPV4_{EC}^{-/-}) knockout mice, we provide the first evidence for a role of AKAP150_{EC}-TRPV4_{EC} channel signaling in modulating resting blood pressure. Moreover, PN formation at the MEPs underlies the specific impairment of AKAP150_{EC}-TRPV4_{EC} channel signaling in obesity, which contributes to obesity-induced loss of endothelium-dependent vasodilation and elevated blood pressure. Spatially localized PN targets AKAP150_{EC} to decrease Ca^{2+} influx through TRPV4_{EC} channels in obesity, an abnormality that is reversed by PN and $\text{O}_2^{\cdot-}$ inhibitors. Our studies implicating dysregulated TRPV4_{EC} channels in defective endothelium-dependent vasodilation in obesity provide a rationale for designing PN-based therapeutics to restore TRPV4_{EC} channel function and normalize blood pressure in obese individuals.

Materials and Methods

The data, analytical methods, and materials are available from the corresponding author upon reasonable request²⁴. An expanded Material and Methods section can be found in the Supplemental Materials.

Animal Models and human tissue

Animal protocols were approved by the University of Virginia Animal Care and Use Committee. Normal or high fat diet-fed (for 14 weeks) C57BL6/J mice, endothelium-specific TRPV4 (TRPV4_{EC}^{-/-}) and AKAP150 (AKAP150_{EC}^{-/-}) knockout mice, and high fat diet-fed TRPV4_{EC}^{-/-} mice were used. Isolation of splenius and temporalis muscle tissue from patients was approved by University of Virginia's Institutional Review Board, and the subjects gave informed consent.

Pressure myography

Arteries were cannulated onto two glass micropipettes on a pressure myography chamber, and pressurized to 80 mm Hg. Internal diameter was recorded in response to various treatments.

Blood pressure measurement

Radiotelemetry catheter was implanted in the left carotid artery under isoflurane anesthesia. Continuous blood pressure measurements were performed following a seven-day recovery period.

Ca²⁺ imaging

Ca²⁺ imaging studies were performed in *en face*, fluo-4-loaded third-order mesenteric arteries (MAs). Images were acquired using a spinning-disk confocal imaging system and electron-multiplying charge coupled device camera.

Peroxyntirite (PN) imaging

Endothelial PN was imaged in *en face* arteries from mice and human samples using PN-selective fluorescent indicator coumarin boronic acid (CBA).

Patch Clamp in ECs and HEK293 cells

Currents through TRPV4 channels and IK/SK channels were recorded in ECs freshly isolated from MAs or HEK293 cells.

Quantitative Polymerase Chain Reaction (qPCR)

RNA was extracted from isolated ECs or MA lysates using Qiagen RNeasy Mini Kit, and cDNA synthesized using Bio-Rad iScript cDNA Synthesis Kit.

Statistics

Data were analyzed using two-tailed, paired or independent t-test, one-way ANOVA (Tukey correction for multiple comparisons), or two-way ANOVA (Bonferroni correction for multiple comparisons). Statistical significance was determined as a *P* value < 0.05.

Results

Endothelium-specific TRPV4- and AKAP150-knockout mice show elevated blood pressure

AKAP150 enhances TRPV4 channel activity via PKC anchoring in multiple cell-types^{15, 16}. It is unclear whether the AKAP150_{EC}-TRPV4_{EC} signaling mechanism impacts blood pressure, since EC-specific knockout of these proteins has not been accomplished to date. Accordingly, we developed and validated two new inducible mouse models, TRPV4_{EC}^{-/-} and AKAP150_{EC}^{-/-}, in which TRPV4 and AKAP150, respectively, were specifically knocked out in ECs. Endothelial knockout of TRPV4 channels or AKAP150 was confirmed by a decrease in TRPV4 and AKAP150 immunostaining in ECs (Figure 1A; Supplemental Figures 1A–1D; Supplemental Table 1), and a decrease in endothelial mRNA for TRPV4 channels and AKAP150 (Figure 1B, Supplemental Figure 1E) in the corresponding knockout models. Unitary Ca²⁺ influx signals through individual TRPV4_{EC} channels, termed TRPV4_{EC} sparklets²⁵, were recorded in resistance mesenteric arteries (MAs) and confirmed by their sensitivity to the highly selective TRPV4 antagonist, GSK2193874 (GSK219, 100 nM; Supplemental Figure 1F). Baseline TRPV4_{EC} sparklet activity (recorded in the presence of 20 μM cyclopiazonic acid [CPA] to eliminate interfering inositol 1,4,5-trisphosphate receptor-mediated Ca²⁺ signals²⁵) as well as that induced by the TRPV4 agonist GSK1016790A (GSK101; 3–30 nM), was markedly reduced in MAs from TRPV4_{EC}^{-/-} mice compared with that in MAs from wild-type (WT) mice (Figure 1C).

The classical muscarinic receptor agonist carbachol (CCh) increases TRPV4_{EC} channel activity in an AKAP150/PKC-dependent manner to promote vasodilation^{10, 15, 25}. In *en face* preparations of MAs from WT mice, AKAP150_{EC} was concentrated mainly at MEPs, identifiable as black holes in the internal elastic lamina (IEL) (Figure 1A; Supplemental Figure 1E). Notably, a spatial localization analysis indicated that baseline TRPV4_{EC} sparklet activity at MEPs, but not at other (non-MEP) sites, was reduced in MAs from AKAP150_{EC}^{-/-} mice compared with WT mice (Figures 1D, 1E; Supplemental Figures 2A, 2B). Moreover, CCh enhanced TRPV4_{EC} sparklet activity only at MEPs, an effect that was not observed in MAs from AKAP150_{EC}^{-/-} mice (Figure 1E; Supplemental Figures 2A, 2B). PKC-mediated activation of TRPV4_{EC} sparklets, induced by the PKC activator PMA (phorbol 12-myristate 13-acetate), also showed a similar AKAP150_{EC}-dependence and localization at MEPs (Supplemental Figures 2B, 2C). Thus, AKAP150_{EC} is required for the activation of TRPV4_{EC} channels at MEPs. Only the direct TRPV4 channel agonist GSK101 (10 nM) was able to increase TRPV4_{EC} sparklet activity in MAs from AKAP150_{EC}^{-/-} mice (Figure 1E). TRPV4_{EC} sparklets represent coupled openings of individual TRPV4_{EC} channels at a given site^{15, 25}. An analysis of cooperative gating among TRPV4_{EC} channels, measured as coupling coefficient (κ) value, which varies from 0 (no coupling or independent gating) to 1 (complete coupling), indicated that coupling was weaker at MEPs in MAs from AKAP150_{EC}^{-/-} mice (Figure 1F; Supplemental Figure 3), supporting a critical role of AKAP150_{EC} in functional coupling of TRPV4_{EC} channels. Furthermore, TRPV4 channel agonist - and CCh-induced dilation of MAs were dramatically decreased in MAs from TRPV4_{EC}^{-/-} and AKAP150_{EC}^{-/-} mice (Figure 1G–1J; Supplemental Figure 4), indicating impaired endothelium-dependent vasodilation in these mice. Importantly, resting systolic, diastolic, and mean arterial pressure (MAP), recorded using radiotelemetry, were elevated in

both TRPV4_{EC}^{-/-} and AKAP150_{EC}^{-/-} mice compared with the respective WT mice (Figure 1K; Supplemental Figure 5). Resting heart rate, however, was not different between WT and knockout mice (Supplemental Figures 5A, 5C). Pressure-induced constriction at 80 mm Hg was higher in both TRPV4_{EC}^{-/-} and AKAP150_{EC}^{-/-} mice compared to respective WT mice (Figure 1L), suggesting higher baseline vascular tone in these mice. These new findings provide initial evidence that AKAP150_{EC}-TRPV4_{EC} signaling at MEPs promotes endothelium-dependent vasodilation and contributes to the regulation of resting blood pressure.

Diet-induced obesity is associated with impaired TRPV4_{EC} sparklet activity and endothelium-dependent vasodilation

Diet-induced obesity caused by excessive intake of energy-dense foods is often accompanied by a rise in blood pressure and defective endothelium-dependent vasodilation^{1, 2}. Here, we explored whether disrupted TRPV4_{EC} Ca²⁺ signaling is a feature of defective endothelium-dependent vasodilation in mice fed a high-fat diet (HFD) for 14 weeks. Body weight of these HFD mice (44 ± 2 g) was significantly higher than that of mice fed a normal-fat diet (NFD; 28 ± 1 g, n = 13; *P* < 0.05, t-test). HFD mice also showed higher resting systolic, diastolic, and MAP (Figure 2A; Supplemental Figures 6A, 6B), and a higher pressure-induced vasoconstriction at 80 mm Hg (Supplemental Figures 6C) compared to NFD mice. CCh-induced, endothelium-dependent dilation was markedly blunted in MAs from HFD mice (Figure 2B). Similarly, dilation of MAs in response to the TRPV4 channel agonist GSK101 was also impaired in HFD mice (Figure 2C). TRPV4_{EC} sparklets activate IK and SK channels to mediate membrane hyperpolarization of ECs, a response that propagates to adjacent SMCs to induce their relaxation and cause dilation of MAs²⁵. In the presence of IK/SK channel inhibitors, there was no significant difference in vasodilation to CCh and GSK101 between NFD and HFD mice (Supplemental Figures 7A, 7B). Moreover, in the presence of 60 mM extracellular K⁺ to inhibit IK/SK channel-mediated hyperpolarization, there was no difference in vasodilation to CCh or GSK101 between NFD and HFD mice (Supplemental Figures 7C–F), further suggesting a specific impairment of TRPV4_{EC}-IK/SK channels in obesity. Conceptually, the loss of TRPV4-mediated vasodilation could be related to reduced expression and/or function of TRPV4_{EC} channels or IK/SK channels. We found that the dilatory response to the IK/SK channel activator NS309 was not altered in MAs from HFD mice (Supplemental Figure 8A), suggesting that the impairment in endothelial function in obesity lies upstream of IK/SK channels, possibly at the level of TRPV4_{EC} channels, and that the communication across MEGJs is not impaired.

Notably, TRPV4_{EC} sparklets were scarce in HFD mice (Figure 2E), a decrease that was spatially restricted to sparklet sites at MEPs (Figures 2E, 2F; Supplemental Figure 8B). Both CCh- and PKC-induced activation of TRPV4_{EC} sparklets, which requires AKAP150_{EC}, was markedly reduced in MAs from HFD mice (Supplemental Figure 8C). Moreover, the AKAP150_{EC}-dependent enhancement of coupling strength among TRPV4_{EC} channels at MEPs was also attenuated in obesity (Supplemental Figure 9A). The quantal level (unitary channel amplitude, reflecting stepwise openings of 1–4 TRPV4 channels at a site²⁵) of TRPV4_{EC} sparklets at MEPs was not altered in AKAP150_{EC}^{-/-} or HFD mice compared with respective controls (Supplemental Figure 9B). Collectively, these findings raise the

possibility of defective AKAP150_{EC} enhancement of TRPV4_{EC} channel function at MEPs in obesity.

Clinical relevance of our findings was established by studying TRPV4_{EC}-mediated vasodilation and TRPV4_{EC} sparklet activity in splenius/temporalis muscle arteries from non-obese and obese individuals. Both CCh and GSK101 dilated the arteries from non-obese individuals, and the vasodilation was absent in the arteries from obese individuals (Figures 2G–J). Moreover, GSK219-sensitive TRPV4_{EC} sparklet activity was attenuated in the arteries from obese individuals when compared to those from non-obese individuals (Figures 2K, 2L). Thus, TRPV4_{EC} channel activity and vasodilation are also impaired in the arteries from obese patients.

Inhibition of NOS or PN restores TRPV4_{EC} channel activity, vasodilation, and blood pressure in obesity

TRPV4_{EC}-IK/SK channel signaling is the major effector pathway for muscarinic receptor signaling-induced dilation of resistance MAs, whereas TRPV4_{EC} channel-independent endothelial NOS (eNOS) activation plays a minor role^{10, 15, 25}. We hypothesized that NOS inhibition would eliminate the residual vasodilation to CCh in obese mice. Surprisingly, NOS inhibition with L-NNA (L-N^G-nitroarginine; 100 μM) restored the vasodilation to both CCh and GSK101 (Figures 3A, 3B) in HFD mice. L-NNA had only a slight inhibitory effect on vasodilation to CCh and no effect on vasodilation to GSK101 in NFD mice (Figures 3A, 3B; Supplemental Figure 10A). L-NNA was unable to rescue the vasodilation to CCh or GSK101 in obese TRPV4_{EC}^{-/-} or AKAP150_{EC}^{-/-} mice (Figures 3A, 3B), suggesting the AKAP150_{EC}-TRPV4_{EC}-dependent rescue of vasodilation by L-NNA in obesity. Moreover, L-NNA rescued TRPV4_{EC} sparklet activity in MAs from HFD mice, but had no effect on TRPV4_{EC} sparklet activity or TRPV4_{EC}-induced vasodilation in NFD mice (Supplemental Figure 10B). NOS-generated NO can react with O₂⁻ radicals to form PN²¹, which is known to have deleterious effects on endothelial function^{23, 26, 27}. O₂⁻ and NO levels were elevated in ECs from HFD mice (Supplemental Figures 11A, 11B). On the basis of these findings, we postulated that PN is the signaling molecule that reduces TRPV4_{EC} sparklet activity in obesity. A PN-selective fluorescent indicator, coumarin boronic acid (CBA), showed a concentration-dependent increase in fluorescence with PN and PN generator SIN-1 (Supplemental Figure 12), and a higher PN fluorescence in ECs from obese patients and mice when compared to respective non-obese controls (Figures 3C, 3D). Using PEG-catalase to decompose H₂O₂ and taurine to scavenge hypochlorous acid did not lower the CBA fluorescence in obese mice, suggesting that H₂O₂ or hypochlorous acid did not contribute to increased CBA fluorescence (Supplemental Figure 13). Moreover, immunostaining for 3-nitrotyrosine (NT), a commonly used biomarker of PN formation, revealed very low levels of 3-NT in MAs from NFD mice, but increased 3-NT formation at MEPs in HFD mice (Supplemental Figure 14). Uric acid (UA; 200 μM) and ebselen (1 μM), PN scavengers²⁸, Fe^{III}-tetra-(4-sulfonatophenyl)-porphyrin (FeTPPs; 1 μM), a PN decomposer²⁹, and tempol (200 μM), a superoxide dismutase (SOD) mimetic that decreases O₂⁻, all rescued TRPV4_{EC} sparklet activity at MEPs in MAs from HFD mice and in the arteries from obese individuals (Figures 3E; Supplemental Figures 15, 16). However, none of these agents affected sparklet activity at non-MEP sites in HFD mice or overall sparklet

activity in MAs of NFD mice (Supplemental Figures 15D–G), pointing to a spatially localized elevation in PN levels at MEPs in obesity.

PN inhibitors UA and FeTPPS also rescued CCh- and PKC-induced activation of TRPV₄^{EC} sparklets in HFD mice, restored coupling coefficients to NFD levels (Supplemental Figure 17A–C) and, like tempol and ebselen, restored dilation to CCh and GSK101 in MAs from HFD mice (Figure 3F; Supplemental Figure 17D). In TRPV₄^{EC}^{-/-} mice or AKAP150^{EC}^{-/-} mice fed a HFD, UA was unable to rescue TRPV₄^{EC} sparklet activity and vasodilation to CCh (Supplemental Figures 17D, 17E), supporting the concept that PN inhibitors specifically rescued AKAP150^{EC}-TRPV₄^{EC}-dependent vasodilation in obesity. Administration of UA (200 mg/kg, i.p.) or FeTPPS (10 mg/kg, i.p.) failed to affect resting blood pressure in NFD mice, but significantly lowered MAP in HFD mice 15 minutes after injection (Figure 3G). Neither compound altered heart rate in HFD mice (Supplemental Figure 18). Moreover, these PN inhibitors had no effect on resting MAP in TRPV₄^{EC}^{-/-} mice fed a HFD (Figure 3G), further confirming that inhibition of PN accumulation restored the ability of TRPV₄^{EC} channels to decrease MAP.

MEP-localized NADPH oxidase 1 (NOX1) and iNOS underlie PN-induced TRPV₄^{EC} channel dysregulation in obesity

NOX activity is a major source of cytosolic O₂⁻ generation in the vasculature³⁰, and both NOX and vascular iNOS activity are increased in obesity¹⁹. Three NOX isoforms—NOX1, NOX2 and NOX4—have been reported in rodent ECs³⁰. In MAs from NFD mice, the predominant NOX isoform detected at MEPs was NOX1 (Figure 4A). Interestingly, the expression of NOX1 at MEPs was increased in MAs from obese mice, whereas expression of NOX2 and NOX4 persisted at low levels (Figure 4A; Supplemental Figures 19, 20). Similarly, expression of iNOS was also elevated at MEPs in MAs from obese mice (Figures 4B, 4C). Consistent with these data, NOX1 and iNOS mRNA levels were elevated in MAs from obese mice compared with NFD mice (Figure 4D). The specific NOX1 inhibitors Nox1ds and ML-171, and iNOS inhibitor, 1400W, restored TRPV₄^{EC} sparklet activity to normal levels at MEPs in MAs from obese mice (Figures 4E–G; Supplemental Figure 21A). However, these compounds had no effect on sparklet activity at non-MEP sites (Figures 4E–G; Supplemental Figure 21A) and failed to affect sparklet activity in MAs from NFD mice (Supplemental Figure 21B). In contrast, the gp91phox blocking peptide, gp91 ds-tat (1 μM), which specifically inhibits NOX2, did not alter TRPV₄^{EC} sparklet activity in obese mice (Supplemental Figure 22). Both NOX1 and iNOS inhibitors restored vasodilator responses to CCh and TRPV₄ agonist in MAs from obese mice (Figures 4H, 4I; Supplemental Figure 23), an effect that was absent in the arteries from HFD TRPV₄^{-/-} mice or HFD AKAP150^{EC}^{-/-} mice (Figures 4H, 4I; Supplemental Figure 24), and lowered the CBA fluorescence in the arteries from obese mice (Supplemental Figure 25). Moreover, 1400W or L-NNA administration also lowered MAP in obese mice (Figure 4J; Supplemental Figure 26). Collectively, these results suggest that elevated NOX1 and iNOS expression at vascular MEPs increases PN formation in obesity, which impairs TRPV₄^{EC} sparklet activity and endothelium-dependent vasodilation.

PN inhibits AKAP150_{EC}-mediated enhancement of TRPV4_{EC} sparklet activity at MEPs

To test whether exogenous PN attenuates TRPV4_{EC} sparklet activity, we exposed MAs from WT mice to either PN (1 μ M) or the PN donor SIN-1 (50 μ M) for 5 minutes. Both PN and SIN-1 decreased TRPV4_{EC} sparklet activity at MEPs, but had no effect on TRPV4_{EC} sparklets at non-MEP sites (Figure 5A; Supplemental Figure 27A). SIN-1 generates NO and O₂⁻, which react to form PN. In the presence of the NO scavenger carboxy-PTIO (50 μ M) or tempol, SIN-1 was unable to inhibit TRPV4_{EC} sparklet activity, indicating that neither O₂⁻ nor NO *per se* alter TRPV4_{EC} sparklet activity (Supplemental Figure 27B). Both UA and FeTPPS inhibited PN-induced 3-NT formation as well as the effect of PN on TRPV4_{EC} sparklet activity at MEPs (Supplemental Figure 28). In patch clamp studies on freshly isolated ECs from WT mice, exogenous PN reduced the currents through TRPV4_{EC} channels (Figure 5B), supporting PN-induced inhibition of channel activity. TRPV4 agonist- and CCh-induced vasodilation was also inhibited in the presence of PN (Figures 5C, 5D; Supplemental Figure 29A). Decomposed PN, however, was unable to impair TRPV4_{EC} sparklet activity or vasodilation (Supplemental Figures 29B–D). Furthermore, both CCh- and PKC-induced (PMA) increases in TRPV4_{EC} sparklet activity were abolished in the presence of PN (Supplemental Figure 30A), and coupling strength among TRPV4_{EC} channels at MEPs was lower in the presence of exogenous PN (Supplemental Figure 30B). Collectively, these findings suggest that PN impairs AKAP150_{EC}-mediated enhancement of TRPV4_{EC} channel activity. Indeed, in MAs from AKAP150_{EC}^{-/-} mice, PN was unable to alter TRPV4_{EC} sparklet activity evoked by TRPV4 agonist (10 nM, Figure 5E), confirming that PN does not directly target the TRPV4_{EC} channel, but instead impairs AKAP150_{EC}-mediated regulation of the channel.

PN-induced cysteine oxidation of AKAP150 lowers TRPV4_{EC} channel activity

Dithiothreitol (DTT; 1 mM), which is used as a reducing agent to reverse cysteine oxidation, rescued TRPV4_{EC} sparklet activity in HFD mice but not in HFD AKAP150_{EC}^{-/-} mice (Supplemental Figure 31), suggesting that PN-induced cysteine oxidation may be responsible for AKAP150_{EC}-TRPV4_{EC} dysfunction in obesity. Ascorbic acid, which is a selective inhibitor of S-nitrosylation³¹, did not alter TRPV4_{EC} sparklet activity in obese mice suggesting that S-nitrosylation may not be responsible for TRPV4_{EC} channel in obesity (Supplemental Figure 32). A 2-thiodimedone antibody to detect cysteine sulfenic acid (CSA) intermediates of cysteine oxidation showed higher CSA levels at MEPs in obese mice when compared to normal mice (Figure 5F). MAs from obese AKAP150_{EC}^{-/-} mice showed minimal CSA staining at MEPs (Figure 5F). Moreover, CSA levels at MEPs in MAs from obese mice were lowered by pretreatment with DTT or PN scavenger UA (Supplemental Figure 33). Overall, these data support the idea that PN causes cysteine oxidation of AKAP150_{EC} in obesity to lower AKAP150_{EC}-TRPV4_{EC} signaling at MEPs.

In HEK293 cells, TRPV4 inhibitor-sensitive currents were increased in the presence of AKAP150 (Figure 5G). Moreover, PN did not alter TRPV4 currents in HEK293 cells expressing TRPV4 channel alone, but did inhibit such currents in cells expressing the TRPV4 channel and AKAP150 (Figure 5G), suggesting that PN decreases TRPV4 channel activity by targeting AKAP150. There is only one cysteine residue (Cys36) in the PKC-binding region (residues 31–52) of AKAP150¹⁴. Substituting Cys36 of AKAP150 with

alanine in HEK293 cells resulted in the loss of PN-inhibition of TRPV4 currents and PN-induced formation of cysteine sulfenic acid, an intermediate in disulfide bond formation (Figure 5G, Supplemental Figure 34). Taken together, these results indicate that PN causes oxidation of Cys36 on AKAP150 to lower TRPV4 channel activity.

TRPV4_{EC} sparklets dilate MAs by activating IK/SK channels^{15, 25}. In freshly isolated ECs, PN did not alter IK/SK currents induced by the direct IK/SK channel activator, NS309 (Supplemental Figure 35A). Furthermore, NS309-induced vasodilation was unaffected by PN (Supplemental Figure 35B), confirming that PN-induced impairment in endothelium-dependent vasodilation occurs upstream of IK/SK channels.

PN impairs AKAP150_{EC}:PKC localization in obesity

The expression of AKAP150_{EC} at MEPs was unaltered in obesity (Figures 6A, 6B), and TRPV4_{EC} and AKAP150_{EC} transcript levels were also unchanged (Figure 6C). We further hypothesized that PN-induced impairment of AKAP150_{EC}-PKC-TRPV4_{EC} signaling in obesity reflects impaired localized coupling of AKAP150_{EC} to PKC and/or TRPV4_{EC}. Proximity ligation assays (PLAs) in MAs from NFD mice indicated that AKAP150_{EC} exists within nanometer proximity of both PKC and TRPV4_{EC} (Figures 6D, 6E). Moreover, AKAP150_{EC}:TRPV4_{EC} localization was not altered in MAs from HFD mice (Figures 6D, 6F). However, we observed less AKAP150_{EC}:PKC localization, suggesting impaired PKC anchoring by AKAP150_{EC} in obesity (Figures 6E, 6F). Therefore, we hypothesized that PN inhibits the anchoring of PKC by AKAP150_{EC} in obesity. Treatment of MAs from obese mice with UA for 5 minutes restored the localization of AKAP150_{EC} with PKC to NFD levels (Figure 6F). Moreover, the PN donor SIN-1 decreased AKAP150_{EC}:PKC localization in WT arteries (Figure 6G). These results support the idea that PN disrupts AKAP150_{EC}-PKC-TRPV4_{EC} vasodilator signaling at MEPs in obesity by specifically inhibiting anchoring of PKC by AKAP150_{EC} (Figure 6H).

Discussion

Using inducible, endothelium-specific knockout mice, we provide the first demonstration of a physiological role for TRPV4_{EC} channels and the regulatory protein AKAP150_{EC} in lowering resting blood pressure. Moreover, we show that increased PN at vascular MEPs targets AKAP150_{EC} and lowers AKAP150_{EC}-mediated enhancement of TRPV4_{EC} channel activity, thereby blunting endothelium-dependent vasodilation and increasing blood pressure in diet-induced obesity. Studies in human arteries establish the clinical relevance of PN-induced impairment of TRPV4_{EC} channels in obesity. Our results further suggest that increased levels of NOX1 and iNOS at vascular MEPs contribute to enhanced formation of PN in obesity, and demonstrate that prevention of PN formation restores AKAP150_{EC}-PKC-TRPV4_{EC} channel vasodilatory signaling (Figure 6H). Thus, our studies lay the foundation for PN-based therapeutic strategies for rescuing TRPV4_{EC} channel function, and thereby improving endothelium-dependent vasodilator responses and lowering blood pressure in obese individuals.

The contribution of TRPV4_{EC} channels to resting blood pressure has been difficult to define. Although numerous studies have identified TRPV4_{EC} channels as a key Ca²⁺ influx pathway

for endothelium-dependent vasodilation, only global TRPV4^{-/-} mice have been available for such studies^{25, 32}. These mice show no change in resting blood pressure^{8, 32}, an observation in stark contrast to the higher blood pressure observed in the TRPV4_{EC}^{-/-} mice developed for the current study. The role of vascular smooth muscle AKAP150-TRPV4 signaling in regulating arterial diameter remains uncertain, with reports linking TRPV4 signaling in this compartment to both vasodilation and vasoconstriction^{16, 33, 34}. Thus, a definitive answer to the questions of how smooth muscle AKAP150-TRPV4 signaling influences blood pressure await the development of SMC-specific TRPV4^{-/-} and AKAP150^{-/-} mice.

An increase in iNOS activity at vascular MEPs contributed to PN formation in obesity, however, higher iNOS levels did not result in vasodilation, a finding that could be explained by the instantaneous reaction of NO with NOX1-generated O₂⁻, thus reducing NO bioavailability. In this regard, NOX1 deletion has previously been shown to lower O₂⁻ levels in a mouse model of metabolic disease³⁵. While our data support the role of NOX1 in obesity-induced PN formation at MEPs, it is not clear whether NOX1 at the cell membrane or intracellular NOX1 or both are responsible for this effect. Importantly, iNOS activity has mainly been associated with immune cells³⁶. Our z-stack images indicate that iNOS upregulation is restricted to MEPs in obesity, and immunostaining for pan-leucocyte marker CD45 revealed that immune cells were not present at the level of IEL in obese mice (Supplemental Figure 36), further supporting the concept that endothelial iNOS contributed to PN formation in obesity. iNOS has been implicated in drastic lowering of blood pressure in sepsis³⁷. It is conceivable that differential mechanisms downstream of iNOS lead to distinct functional effects in obesity and sepsis.

Although several endogenous oxidant molecules can cause cysteine oxidation^{38, 39}, AKAP150_{EC}-TRPV4_{EC} channel impairment in obesity can be attributed specifically to PN-induced cysteine oxidation of AKAP150_{EC}. We show that PEG-catalase and taurine are unable to rescue TRPV4_{EC} sparklet activity or vasodilation in obese mice (Supplemental Figure 37), suggesting that H₂O₂ or hypochlorous acid do not play a major role in obesity-induced impairment of TRPV4_{EC} channels. Interestingly, addition of high concentration of exogenous H₂O₂, but not hypochlorous acid, lowered TRPV4_{EC} sparklet activity in MAs from normal mice (Supplemental Figure 38), although the mechanism for this effect is not known. Superoxide and NO radicals have also been commonly associated with cysteine modifications⁴⁰. Using the hypoxanthine/xanthine oxidase system, we observed that superoxide radicals inhibited vasodilation to CCh in normal mice, but had no effect on TRPV4_{EC} sparklet activity (Supplemental Figure 39). Thus, superoxide radicals are not directly responsible for impairing TRPV4_{EC} channel activity in obesity. Moreover, NO donor spermine NONOate (100 μM) also inhibited TRPV4_{EC} sparklet activity²⁴ (Supplemental Figure 40), however, this effect was previously attributed to the activation of endothelial guanylyl cyclase-protein kinase G pathway²⁴.

Cysteine modifications have a short half-life⁴¹, which may explain the restoration of AKAP150_{EC}-TRPV4_{EC} signaling within five minutes in obesity. It is plausible that lowering PN levels allows the endogenous glutaredoxins, thioredoxins, and/or peroxiredoxins to reduce oxidized cysteines on AKAP150_{EC}⁴². PN may also lead to S-nitrosation, however, treatment with ascorbic acid was unable to rescue TRPV4_{EC} channel activity in obesity.

While a lack of response to ascorbic acid does not definitively exclude a role for S-nitrosothiols, this result together with the detection of cysteine oxidation of AKAP150_{EC} support thiol oxidation as the primary mechanism impairing AKAP150_{EC}-TRPV4_{EC} signaling in obesity. PN may also cause cysteine oxidation of PKC, which is known for its redox regulation⁴³. However, preventing Cys36 oxidation of AKAP150 alone was sufficient to abolish the effect of PN on TRPV4_{EC} channel activity, suggesting that PN-induced thiol oxidation of PKC may not play a role in obesity-induced loss of endothelial function.

Exogenously applied PN has been shown to have varying effects on vascular diameter^{44, 45}. We observed that PN (5 μ M) caused a slight and transient vasodilation that was similar to that caused by 100 nM spermine NONOate (Supplemental Figures 41A, 41B). However, NONOate did not alter the vasodilation to CCh or TRPV4_{EC} sparklet activity at this concentration (Supplemental Figures 41C, 41D). It should be noted that the effect of exogenously applied PN on vascular diameter is likely an integral of its effects in multiple cell types including smooth muscle cells, and could be different from the effect of locally formed PN in ECs during obesity.

While obesity is a significant risk factor for cardiovascular abnormalities in both sexes, obese female mice did not show a loss of endothelium-dependent vasodilation (Supplemental Figure 42). The risk of hypertension is known to be more in men than women at young ages⁴⁶, a trend that is reversed post-menopause. It is plausible that estrogen has a beneficial effect on endothelial function during obesity⁴⁷. Future studies on endothelial dysfunction in obese female mice are needed to address a significant health concerns of obesity-induced hypertension in women.

A recent study supported a key role for perivascular adipose tissue (PVAT) in NO generation and vasodilation⁴⁸. Moreover, obesity was shown to be associated with uncoupling of eNOS from PVAT in obesity⁴⁹. Therefore, it is plausible that NO/superoxide radicals generated in PVAT contribute to PN formation and endothelial dysfunction. PVAT can also release inflammatory cytokines³⁶ that may elevate iNOS and NOX1 levels in ECs, thereby having a long-term effect on endothelial function. However, PVAT was cleaned off for all the *ex vivo* experiments in this study, thus, obesity-induced effects on TRPV4_{EC} channel activity and vasodilation were independent of PVAT in the current study.

In conclusion, iNOS-generated NO can react with NOX1-generated superoxide to have deleterious effects on vasodilation under pathological conditions. A localized elevation in PN levels at vascular MEPs appears to be sufficient to decrease AKAP150_{EC}-mediated enhancement of TRPV4_{EC} channel activity without affecting the expression of AKAP150_{EC} or TRPV4_{EC} channels. Although reactive oxygen and nitrogen species have been implicated in hypertension, results presented here identify specific signaling mechanisms that could be therapeutically targeted for rescuing endothelium-dependent vasodilation and blood pressure in obesity.

Supplementary Material

Refer to Web version on PubMed Central for supplementary material.

Acknowledgments

Funding Sources

This work was supported by grants from the National Institutes of Health to SKS (HL142808, HL146914, HL138496) and BEI (HL088554), and American Heart Association to KH (18POST33960212).

Non-standard Abbreviations and Acronyms

EC	Endothelial Cell
ER	Endoplasmic Reticulum
TRPV4_{EC}	Endothelial cell transient receptor potential vanilloid 4 channel
SMCs	Smooth muscle cells
MEPs	Myoendothelial projections
IK	Intermediate-conductance calcium-sensitive potassium channels
SK	Small-conductance calcium-sensitive potassium channels
MEGJs	Myoendothelial gap junctions
AKAP150	A-kinase anchoring protein 150
PKA	Protein kinase A
PKC	Protein kinase C
ROS	Reactive oxygen species
NO	Nitric oxide
iNOS	Inducible nitric oxide synthase
PN	Peroxynitrite
TRPV4_{EC}^{-/-}	Endothelial cell-specific TRPV4 knockout
AKAP150_{EC}^{-/-}	Endothelial cell-specific AKAP150 knockout
MA	Mesenteric artery
CBA	Coumarin boronic acid
ANOVA	Analysis of variance
CPA	Cyclopiazonic acid
WT	Wild-type
CCh	Carbachol

IEL	Internal elastic lamina
MAP	Mean arterial pressure
HFD	High fat diet
NFD	Normal fat diet
eNOS	Endothelial nitric oxide synthase
L-NNA	L-N ^G -nitroarginine
NT	3-nitrotyrosine
UA	Uric acid
SOD	Superoxide dismutase
NOX	NADPH oxidase
DTT	Dithiothreitol
CSA	Cysteine sulfenic acid
PVAT	Perivascular adipose tissue

References

- Hall JE, do Carmo JM, da Silva AA, Wang Z and Hall ME. Obesity-induced hypertension: interaction of neurohumoral and renal mechanisms. *Circ Res.* 2015;116:991–1006. [PubMed: 25767285]
- DeMarco VG, Aroor AR and Sowers JR. The pathophysiology of hypertension in patients with obesity. *Nat Rev Endocrinol.* 2014;10:364–376. [PubMed: 24732974]
- Campia U, Tesaro M and Cardillo C. Human obesity and endothelium-dependent responsiveness. *Br J Pharmacol.* 2012;165:561–573. [PubMed: 21895631]
- Sasaki S, Higashi Y, Nakagawa K, Kimura M, Noma K, Sasaki S, Hara K, Matsuura H, Goto C, Oshima T and Chayama K. A low-calorie diet improves endothelium-dependent vasodilation in obese patients with essential hypertension. *Am J Hypertens.* 2002;15:302–309. [PubMed: 11991214]
- Candela J, Wang R and White C. Microvascular Endothelial Dysfunction in Obesity Is Driven by Macrophage-Dependent Hydrogen Sulfide Depletion. *Arterioscler Thromb Vasc Biol.* 2017;37:889–899. [PubMed: 28336559]
- Korda M, Kubant R, Patton S and Malinski T. Leptin-induced endothelial dysfunction in obesity. *Am J Physiol Heart Circ Physiol.* 2008;295:H1514–21. [PubMed: 18689498]
- Ottolini M, Hong K and Sonkusare SK. Calcium signals that determine vascular resistance. *Wiley Interdiscip Rev Syst Biol Med.* 2019:e1448. [PubMed: 30884210]
- Hong K, Cope EL, DeLalio LJ, Marziano C, Isakson BE and Sonkusare SK. TRPV4 (Transient Receptor Potential Vanilloid 4) Channel-Dependent Negative Feedback Mechanism Regulates Gq Protein-Coupled Receptor-Induced Vasoconstriction. *Arterioscler Thromb Vasc Biol.* 2018;38:542–554. [PubMed: 29301784]
- Sullivan MN, Gonzales AL, Pires PW, Bruhl A, Leo MD, Li W, Oulidi A, Boop FA, Feng Y, Jaggar JH, Welsh DG and Earley S. Localized TRPA1 channel Ca²⁺ signals stimulated by reactive oxygen species promote cerebral artery dilation. *Sci Signal.* 2015;8:ra2. [PubMed: 25564678]

10. Bagher P, Beleznai T, Kansui Y, Mitchell R, Garland CJ and Dora KA. Low intravascular pressure activates endothelial cell TRPV4 channels, local Ca²⁺ events, and IKCa channels, reducing arteriolar tone. *Proc Natl Acad Sci U S A*. 2012;109:18174–18179. [PubMed: 23071308]
11. Dora KA, Sandow SL, Gallagher NT, Takano H, Rummery NM, Hill CE and Garland CJ. Myoendothelial gap junctions may provide the pathway for EDHF in mouse mesenteric artery. *Journal of Vascular Research*. 2003;40:480–490. [PubMed: 14583659]
12. Sandow SL, Tare M, Coleman HA, Hill CE and Parkington HC. Involvement of myoendothelial gap junctions in the actions of endothelium-derived hyperpolarizing factor. *Circ Res*. 2002;90:1108–1113. [PubMed: 12039801]
13. Dell'Acqua ML and Scott JD. Protein kinase A anchoring. *J Biol Chem*. 1997;272:12881–4. [PubMed: 9190362]
14. Faux MC, Rollins EN, Edwards AS, Langeberg LK, Newton AC and Scott JD. Mechanism of A-kinase-anchoring protein 79 (AKAP79) and protein kinase C interaction. *Biochem J*. 1999;343 Pt 2:443–452. [PubMed: 10510312]
15. Sonkusare SK, Dalsgaard T, Bonev AD, Hill-Eubanks DC, Kotlikoff MI, Scott JD, Santana LF and Nelson MT. AKAP150-dependent cooperative TRPV4 channel gating is central to endothelium-dependent vasodilation and is disrupted in hypertension. *Sci Signal*. 2014;7:ra66. [PubMed: 25005230]
16. Mercado J, Baylie R, Navedo MF, Yuan C, Scott JD, Nelson MT, Brayden JE and Santana LF. Local control of TRPV4 channels by AKAP150-targeted PKC in arterial smooth muscle. *J Gen Physiol*. 2014;143:559–575. [PubMed: 24778429]
17. Silver AE, Beske SD, Christou DD, Donato AJ, Moreau KL, Eskurza I, Gates PE and Seals DR. Overweight and obese humans demonstrate increased vascular endothelial NAD(P)H oxidase-p47(phox) expression and evidence of endothelial oxidative stress. *Circulation*. 2007;115:627–637. [PubMed: 17242275]
18. Lynch CM, Kinzenbaw DA, Chen X, Zhan S, Mezzetti E, Filosa J, Ergul A, Faulkner JL, Faraci FM and Didion SP. Nox2-derived superoxide contributes to cerebral vascular dysfunction in diet-induced obesity. *Stroke*. 2013;44:3195–3201. [PubMed: 24072007]
19. Noronha BT, Li JM, Wheatcroft SB, Shah AM and Kearney MT. Inducible nitric oxide synthase has divergent effects on vascular and metabolic function in obesity. *Diabetes*. 2005;54:1082–1089. [PubMed: 15793247]
20. Soares AG, de Carvalho MHC and Akamine E. Obesity Induces Artery-Specific Alterations: Evaluation of Vascular Function and Inflammatory and Smooth Muscle Phenotypic Markers. *Biomed Res Int*. 2017;2017:5038602. [PubMed: 28466012]
21. Peroxynitrite Radi R., a stealthy biological oxidant. *J Biol Chem*. 2013;288:26464–72. [PubMed: 23861390]
22. Brodsky SV, Gealekman O, Chen J, Zhang F, Togashi N, Crabtree M, Gross SS, Nasjletti A and Goligorsky MS. Prevention and reversal of premature endothelial cell senescence and vasculopathy in obesity-induced diabetes by ebselen. *Circ Res*. 2004;94:377–384. [PubMed: 14670841]
23. Cassuto J, Dou H, Czikora I, Szabo A, Patel VS, Kamath V, Belin de Chantemele E, Feher A, Romero MJ and Bagi Z. Peroxynitrite disrupts endothelial caveolae leading to eNOS uncoupling and diminished flow-mediated dilation in coronary arterioles of diabetic patients. *Diabetes*. 2014;63:1381–1393. [PubMed: 24353182]
24. Marziano C, Hong K, Cope EL, Kotlikoff MI, Isakson BE and Sonkusare SK. Nitric Oxide-Dependent Feedback Loop Regulates Transient Receptor Potential Vanilloid 4 (TRPV4) Channel Cooperativity and Endothelial Function in Small Pulmonary Arteries. *J Am Heart Assoc*. 2017;6.
25. Sonkusare SK, Bonev AD, Ledoux J, Liedtke W, Kotlikoff MI, Heppner TJ, Hill-Eubanks DC and Nelson MT. Elementary Ca²⁺ signals through endothelial TRPV4 channels regulate vascular function. *Science*. 2012;336:597–601. [PubMed: 22556255]
26. Knepler JL Jr., Taher LN, Gupta MP, Patterson C, Pavalko F, Ober MD and Hart CM. Peroxynitrite causes endothelial cell monolayer barrier dysfunction. *Am J Physiol Cell Physiol*. 2001;281:C1064–C1075. [PubMed: 11502585]

27. Wattanapitayakul SK, Weinstein DM, Holycross BJ and Bauer JA. Endothelial dysfunction and peroxynitrite formation are early events in angiotensin-induced cardiovascular disorders. *FASEB J*. 2000;14:271–278. [PubMed: 10657983]
28. Skinner KA, White CR, Patel R, Tan S, Barnes S, Kirk M, Darley-Usmar V and Parks DA. Nitrosation of uric acid by peroxynitrite. Formation of a vasoactive nitric oxide donor. *J Biol Chem*. 1998;273:24491–24497. [PubMed: 9733742]
29. Kumar A, Chen SH, Kadiiska MB, Hong JS, Zielonka J, Kalyanaraman B and Mason RP. Inducible nitric oxide synthase is key to peroxynitrite-mediated, LPS-induced protein radical formation in murine microglial BV2 cells. *Free Radic Biol Med*. 2014;73:51–59. [PubMed: 24746617]
30. Drummond GR and Sobey CG. Endothelial NADPH oxidases: which NOX to target in vascular disease? *Trends Endocrinol Metab*. 2014;25:452–463. [PubMed: 25066192]
31. Oh CK, Sultan A, Platzer J, Dolatabadi N, Soldner F, McClatchy DB, Diedrich JK, Yates JR 3rd, Ambasudhan R, Nakamura T, Jaenisch R and Lipton SA. S-Nitrosylation of PINK1 Attenuates PINK1/Parkin-Dependent Mitophagy in hiPSC-Based Parkinson's Disease Models. *Cell Rep*. 2017;21:2171–2182. [PubMed: 29166608]
32. Zhang DX, Mendoza SA, Bubolz AH, Mizuno A, Ge ZD, Li R, Warltier DC, Suzuki M and Gutterman DD. Transient receptor potential vanilloid type 4-deficient mice exhibit impaired endothelium-dependent relaxation induced by acetylcholine in vitro and in vivo. *Hypertension*. 2009;53:532–538. [PubMed: 19188524]
33. Earley S, Heppner TJ, Nelson MT and Brayden JE. TRPV4 forms a novel Ca²⁺ signaling complex with ryanodine receptors and BKCa channels. *Circ Res*. 2005;97:1270–1279. [PubMed: 16269659]
34. Xia Y, Fu Z, Hu J, Huang C, Paudel O, Cai S, Liedtke W and Sham JS. TRPV4 channel contributes to serotonin-induced pulmonary vasoconstriction and the enhanced vascular reactivity in chronic hypoxic pulmonary hypertension. *Am J Physiol Cell Physiol*. 2013;305:C704–C715. [PubMed: 23739180]
35. Thompson JA, Larion S, Mintz JD, Belin de Chantemele EJ, Fulton DJ and Stepp DW. Genetic Deletion of NADPH Oxidase 1 Rescues Microvascular Function in Mice With Metabolic Disease. *Circ Res*. 2017;121:502–511. [PubMed: 28684629]
36. Bogdan C Nitric oxide synthase in innate and adaptive immunity: an update. *Trends Immunol*. 2015;36:161–178. [PubMed: 25687683]
37. MacMicking JD, Nathan C, Hom G, Chartrain N, Fletcher DS, Trumbauer M, Stevens K, Xie QW, Sokol K, Hutchinson N and et al. Altered responses to bacterial infection and endotoxic shock in mice lacking inducible nitric oxide synthase. *Cell*. 1995;81:641–650. [PubMed: 7538909]
38. Nelson KJ, Bolduc JA, Wu H, Collins JA, Burke EA, Reisz JA, Klomsiri C, Wood ST, Yammani RR, Poole LB, Furdul CM and Loeser RF. H₂O₂ oxidation of cysteine residues in c-Jun N-terminal kinase 2 (JNK2) contributes to redox regulation in human articular chondrocytes. *J Biol Chem*. 2018;293:16376–16389. [PubMed: 30190325]
39. Peskin AV and Winterbourn CC. Kinetics of the reactions of hypochlorous acid and amino acid chloramines with thiols, methionine, and ascorbate. *Free Radic Biol Med*. 2001;30:572–579. [PubMed: 11182528]
40. Cardey B, Foley S and Enescu M. Mechanism of thiol oxidation by the superoxide radical. *J Phys Chem A*. 2007;111:13046–13052. [PubMed: 18044848]
41. Wani R and Murray BW. Analysis of Cysteine Redox Post-Translational Modifications in Cell Biology and Drug Pharmacology. *Methods Mol Biol*. 2017;1558:191–212. [PubMed: 28150239]
42. Hanschmann EM, Godoy JR, Berndt C, Hudemann C and Lillig CH. Thioredoxins, glutaredoxins, and peroxiredoxins--molecular mechanisms and health significance: from cofactors to antioxidants to redox signaling. *Antioxid Redox Signal*. 2013;19:1539–1605. [PubMed: 23397885]
43. Steinberg SF. Mechanisms for redox-regulation of protein kinase C. *Front Pharmacol*. 2015;6:128. [PubMed: 26157389]
44. Brzezinska AK, Gebremedhin D, Chilian WM, Kalyanaraman B and Elliott SJ. Peroxynitrite reversibly inhibits Ca(2+)-activated K(+) channels in rat cerebral artery smooth muscle cells. *Am J Physiol Heart Circ Physiol*. 2000;278:H1883–H1890. [PubMed: 10843885]

45. Ohashi M, Faraci F and Heistad D. Peroxynitrite hyperpolarizes smooth muscle and relaxes internal carotid artery in rabbit via ATP-sensitive K⁺ channels. *Am J Physiol Heart Circ Physiol*. 2005;289:H2244–H2250. [PubMed: 16219814]
46. Faulkner JL and Belin de Chantemele EJ. Sex Differences in Mechanisms of Hypertension Associated With Obesity. *Hypertension*. 2018;71:15–21. [PubMed: 29133358]
47. Iorga A, Cunningham CM, Moazeni S, Ruffenach G, Umar S and Eghbali M. The protective role of estrogen and estrogen receptors in cardiovascular disease and the controversial use of estrogen therapy. *Biol Sex Differ*. 2017;8:33. [PubMed: 29065927]
48. Gil-Ortega M, Stucchi P, Guzman-Ruiz R, Cano V, Arribas S, Gonzalez MC, Ruiz-Gayo M, Fernandez-Alfonso MS and Somoza B. Adaptive nitric oxide overproduction in perivascular adipose tissue during early diet-induced obesity. *Endocrinology*. 2010;151:3299–3306. [PubMed: 20410199]
49. Xia N, Horke S, Habermeier A, Closs EI, Reifenberg G, Gericke A, Mikhed Y, Munzel T, Daiber A, Forstermann U and Li H. Uncoupling of Endothelial Nitric Oxide Synthase in Perivascular Adipose Tissue of Diet-Induced Obese Mice. *Arterioscler Thromb Vasc Biol*. 2016;36:78–85. [PubMed: 26586660]

What is new?

- Inducible, endothelium-specific TRPV4 channel or AKAP150 knockout mice show higher resting blood pressures.
- Obesity-induced impairment of endothelial AKAP150-TRPV4 channel signaling contributes to the loss of endothelial function and elevated blood pressure.
- Lowering the levels of oxidant molecule peroxynitrite rescues endothelial AKAP150-TRPV4 channel signaling, vasodilation, and blood pressure in obesity.
- Upregulation of endothelial NOX1 and iNOS increases peroxynitrite formation close to endothelial AKAP150 in obesity.
- Peroxynitrite causes cysteine oxidation of endothelial AKAP150, resulting in the impairment of AKAP150-TRPV4 channel signaling in obesity.

What are the clinical implications?

- Endothelial TRPV4 channels are essential regulators of resting blood pressure, and impairment of endothelial TRPV4 channel activity contributes to obesity-induced hypertension.
- Therapeutic strategies that lower peroxynitrite levels can be used to rescue endothelial TRPV4 channel activity, endothelial function, and blood pressure in obesity.

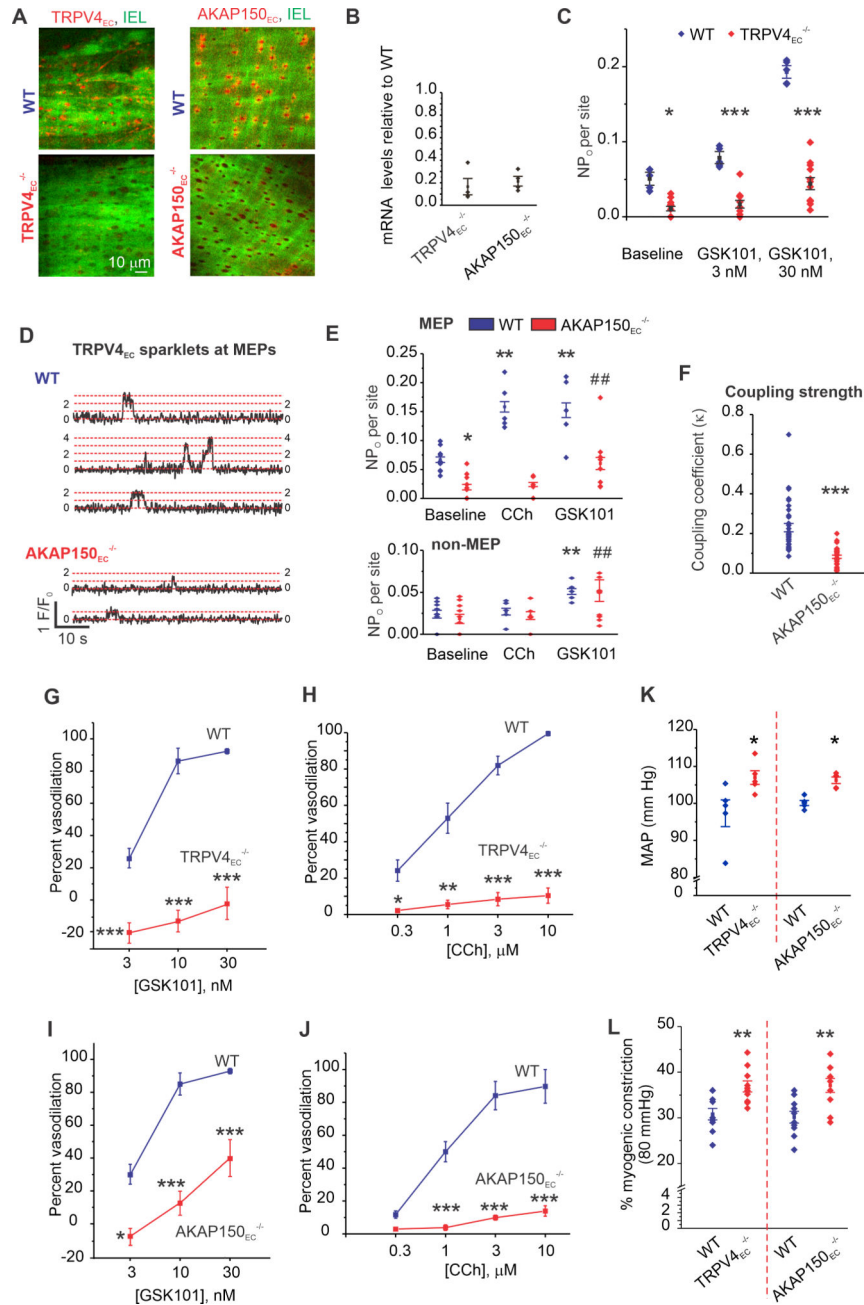


Figure 1. Endothelium-specific TRPV4 ($TRPV4_{EC}^{-/-}$) and AKAP150 ($AKAP150_{EC}^{-/-}$) knockout mice show elevated resting blood pressure.

(A) Representative merged images from *en face* preparations of third-order MAs showing IEL autofluorescence (green) and TRPV4_{EC} or AKAP150_{EC} immunofluorescence (red) in WT (*top*), and TRPV4_{EC}^{-/-} or AKAP150_{EC}^{-/-} (*bottom*) mice. (B) Relative TRPV4 and AKAP150 mRNA levels in ECs from TRPV4_{EC}^{-/-} and AKAP150_{EC}^{-/-} mice, respectively, relative to those in WT mice ($P < 0.01$ for TRPV4_{EC}^{-/-} or AKAP150_{EC}^{-/-} mice vs. respective WT mice; $n=4$; $***P < 0.001$; t-test). (C) TRPV4_{EC} sparklet activity per site (NP_0) in *en face* preparations of MAs from WT and TRPV4_{EC}^{-/-} mice under baseline conditions (i.e., 20 μ M CPA) or in response to 3 and 10 nM GSK101 ($n = 5-11$; $*P < 0.05$

[baseline], <0.001 [3 nM GSK101] and <0.001 [30 nM GSK101] for WT vs. TRPV4_{EC}^{-/-}; one-way ANOVA). (D) Representative baseline F/F₀ traces from TRPV4_{EC} sparklet sites at MEPS in Fluo-4-loaded MAs from WT (*top*) and AKAP150_{EC}^{-/-} (*bottom*) mice. Dotted red lines indicate quantal levels²⁵ derived from an all-points histogram (Extended Data Fig. 7). (E) TRPV4_{EC} sparklet activity at MEP (*top*) and non-MEP (*bottom*) sites in MAs from WT and AKAP150_{EC}^{-/-} mice under baseline conditions, and following treatment with 10 μM CCh or 10 nM GSK101 (n = 5; $P < 0.05$ for WT baseline vs. TRPV4_{EC}^{-/-} baseline, $** < 0.01$ for WT CCh vs. WT baseline, < 0.01 for WT GSK101 vs. WT baseline; $^{##} P < 0.01$ for AKAP150_{EC}^{-/-} GSK101 vs. AKAP150_{EC}^{-/-} baseline; one-way ANOVA). (F) Coupling coefficient (κ) values for TRPV4_{EC} sparklet sites at MEPS indicating the coupling strength among TRPV4_{EC} channels at a given site in MAs from AKAP150_{EC}^{-/-} and WT mice ($P < 0.001$, t-test, n = 25–31 sites). (G) Averaged data for GSK101-induced dilation of MAs from WT and TRPV4_{EC}^{-/-} mice (n = 5; $P < 0.01$ [3 nM GSK101], < 0.001 [10 nM GSK101] and < 0.001 [30 nM GSK101] for WT vs. TRPV4_{EC}^{-/-} mice; two-way ANOVA). (H) Percent dilation of MAs from WT and TRPV4_{EC}^{-/-} mice in response to CCh (0.3–10 μM) (n = 5; $P < 0.05$ [0.3 μM CCh] and < 0.001 [1, 3, and 10 μM CCh] for WT vs. TRPV4_{EC}^{-/-} mice; two-way ANOVA). (I) Percent dilation of MAs from WT and AKAP150_{EC}^{-/-} mice in response to GSK101 (3–30 nM) (n = 5–6; $P < 0.05$ [3 nM GSK101], < 0.01 [10 nM GSK101] and < 0.001 [30 nM GSK101] for WT vs. AKAP150_{EC}^{-/-} mice; two-way ANOVA). (J) Percent dilation of MAs from WT and AKAP150_{EC}^{-/-} mice in response to CCh (0.3–10 μM) (n = 5; $P < 0.05$ [0.3 μM CCh] and < 0.001 [1, 3, and 10 μM CCh] for WT vs. AKAP150_{EC}^{-/-} mice; two-way ANOVA). (K) Scatter plot of resting MAP (mm Hg) averaged over 3 days in TRPV4_{EC}^{-/-} and AKAP150_{EC}^{-/-} mice and the respective WT mice ($P < 0.01$ for TRPV4_{EC}^{-/-} vs. WT mice, $P < 0.05$ for AKAP150_{EC}^{-/-} vs. WT mice; t-test, n=5). (L) Percent myogenic constriction at 80 mm Hg in MAs from TRPV4_{EC}^{-/-} and AKAP150_{EC}^{-/-}, and respective WT mice ($P < 0.01$ vs. WT, t-test, n=10).

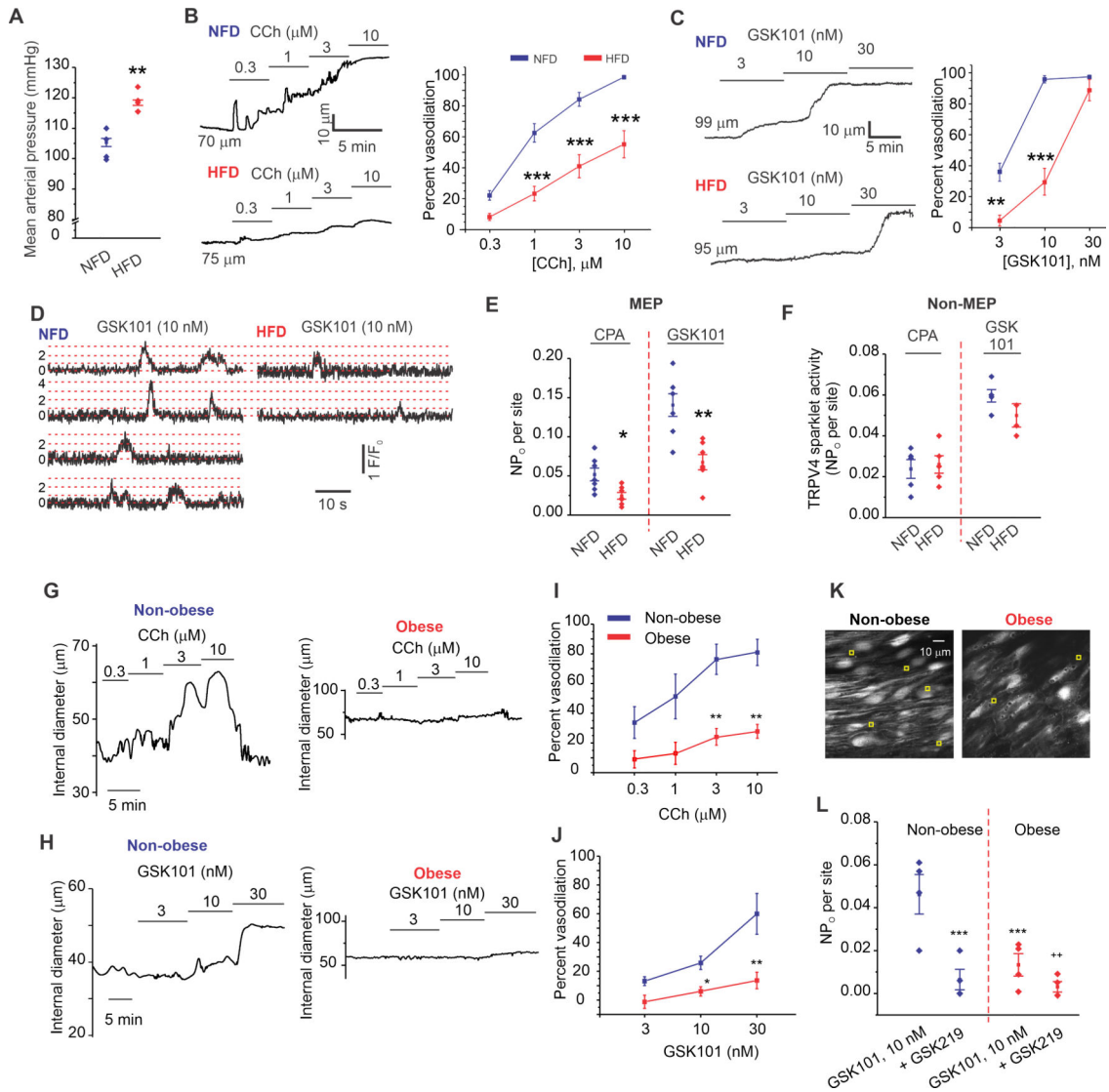


Figure 2. Diet-induced obesity impairs AKAP150_{EC}-PKC-TRPV4_{EC} signaling and vasodilation. (A) Resting MAP (mm Hg) averaged over 3 days in HFD and NFD mice (n = 5; ***P* < 0.01 for HFD vs. NFD; t-test). (B) Representative diameter traces (*left*) and averaged diameter data (*right*) for CCh (0.3–10 μM)-induced dilation of MAs from NFD and HFD mice (n = 8–11; ****P* < 0.001 for 1 μM, 3 μM, and 10 μM CCh for NFD vs. HFD mice; two-way ANOVA). (C) Representative diameter traces (*left*) and averaged diameter data (*right*) for GSK101 (3–30 nM)-induced vasodilation in NFD and HFD mice (n = 5–9; *P* < 0.01 [3 nM GSK101] and < 0.001 [10 nM GSK101]; two-way ANOVA). (D) Representative F/F₀ traces from TRPV4_{EC} sparklet sites (20 μM CPA + GSK101, 10 nM) at MEPs in Fluo-4–loaded *en face* preparations of MAs from NFD (*left*) and HFD (*right*) mice. Dotted red lines indicate quantal levels. (E) Averaged TRPV4_{EC} sparklet activity (NP₀) at MEPs in MAs from NFD and HFD mice under baseline conditions (20 μM CPA) or in response to GSK101 (10 nM) (n = 7; sparklet activity: **P* < 0.05 [CPA] and < 0.01 [GSK101] for NFD vs. HFD). (F) Averaged TRPV4_{EC} sparklet activity in MAs from NFD and HFD mice under baseline conditions (20 μM CPA) and in response to GSK101 (10 nM) (n = 7). (G) Representative

diameter traces for CCh (0.3–10 μM)-induced dilation of splenius muscle arteries from non-obese and obese individuals. (H) Representative diameter traces for GSK101 (3–30 nM)-induced dilation of splenius muscle arteries from obese and non-obese individuals. (I) Averaged diameter data for CCh -induced vasodilation in human splenius and temporalis muscle arteries from obese and non-obese individuals ($n = 6$; $P < 0.01$ vs. non-obese; two-way ANOVA). (J) Averaged diameter data for GSK101-induced vasodilation in human splenius and temporalis muscle arteries from obese and non-obese individuals ($n = 6$; $P < 0.01$, < 0.01 , vs. non-obese; two-way ANOVA). (K) Greyscale image of a field of view with ~ 20 ECs from an *en face* preparation of Fluo-4 loaded splenius muscle artery (SMA) from a non-obese individual; yellow squares indicate sparklet sites in with CPA + GSK101 (10 nM). (L) TRPV4_{EC} sparklet activity (NP_O) at MEP in SMAs from non-obese and obese individuals in response to GSK101 (10 nM) and in the presence of GSK219 (100 nM) ($n = 4$; $P < 0.001$ [GSK101] for non-obese vs. obese and $P < 0.01$ [GSK101] vs. [GSK219]; one-way ANOVA).

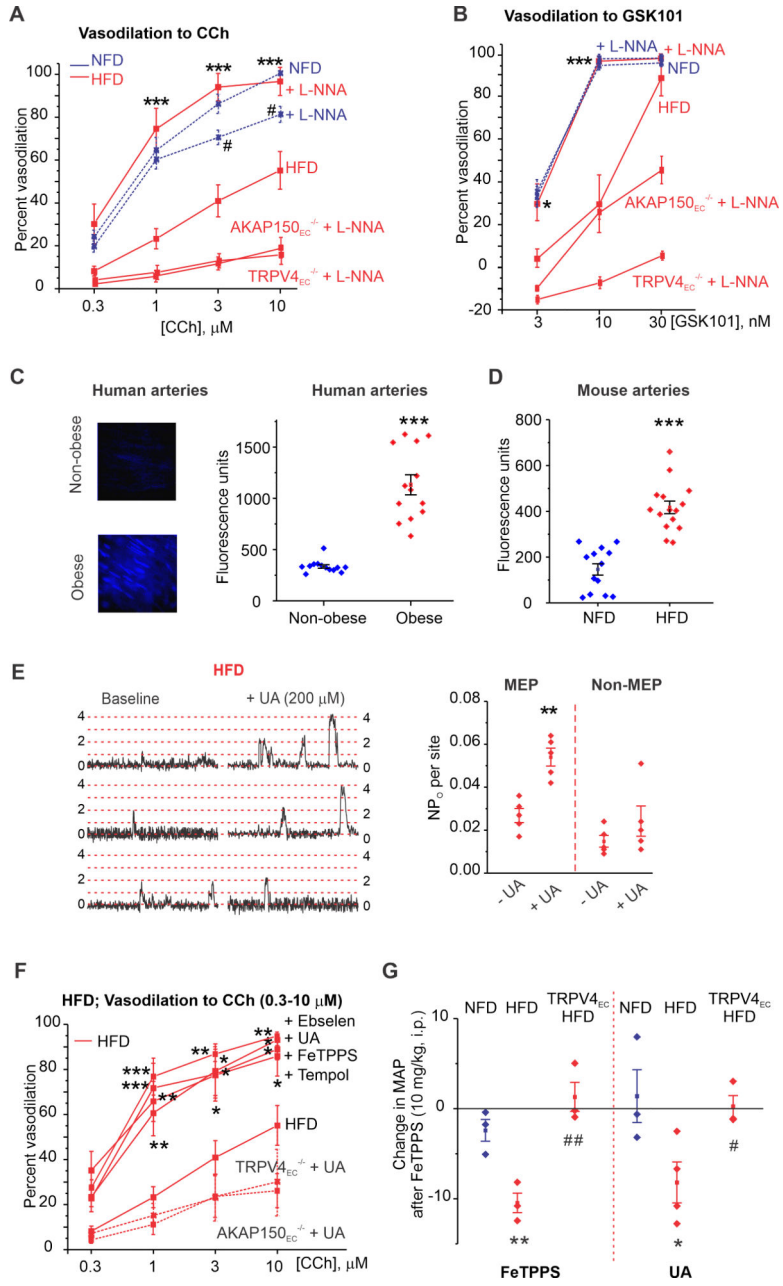


Figure 3. Elevation of endothelial peroxynitrite (PN) impairs TRPV4_{EC} channel activity in obesity.

(A) Percent dilation of MAs from NFD, HFD, HFD AKAP150_{EC}^{-/-}, and HFD TRPV4_{EC}^{-/-} mice in response to CCh (0.3–10 μM) in the presence or absence of L-NNA (100 μM) (n = 5–9; #*P*<0.05 [3 and 10 μM CCh] for NFD vs. NFD + L-NNA; ****P*< 0.001 [1, 3, and 10 μM CCh] for HFD vs. HFD + L-NNA; two-way ANOVA). (B) Percent dilation of MAs from NFD, HFD, HFD AKAP150_{EC}^{-/-}, and HFD TRPV4_{EC}^{-/-} mice in response to GSK101 (3–30 nM) in the presence or absence of L-NNA (100 μM) (n = 5; **P*< 0.05 at 3 nM GSK101 and < 0.001 at 10 nM GSK101 for HFD vs. HFD + L-NNA; two-way ANOVA). (C) Representative images for CBA fluorescence in ECs of splenius muscle arteries from non-

obese (*top-left*) and obese (*bottom-left*) individuals; scatter plot of CBA fluorescence intensity (*right*) in ECs from non-obese and obese patients ($P < 0.001$; $n = 12$ fields from 3 arteries; t-test). (D) CBA fluorescence intensity in ECs of MAs from NFD and HFD mice ($P < 0.001$; $n = 13\text{--}15$ fields from 3 arteries; t-test). (E) Representative F/F_0 traces (*left*) and scatter plot of TRPV₄EC sparklet activity (*right*) from MEP and non-MEP sites in fluo-4-loaded MAs from HFD mice in the absence or presence of UA (200 μM) ($n = 5$; $P < 0.01$ for MEP sites with vs. without UA; one-way ANOVA). Dotted red lines indicate quantal levels. (F) Effects of UA (200 μM), FeTPPS (1 μM), tempol (200 μM), and Ebselen (1 μM) on CCh (0.3–10 μM)-induced dilation of MAs from HFD mice (WT), TRPV₄EC^{-/-} HFD, and AKAP150_{EC}^{-/-} HFD mice ($n = 5\text{--}8$; $P < 0.05$; < 0.01 ; < 0.001 vs. HFD only; two-way ANOVA). (G) Changes in resting MAP (mm Hg) in NFD and HFD mice following i.p. injection of FeTPPS (10 mg/kg; *left*) ($n = 3\text{--}4$; $P < 0.01$ for FeTPPS-treated NFD vs. FeTPPS-treated HFD, $^{##}P < 0.01$ for FeTPPS-treated HFD vs. FeTPPS-treated TRPV₄EC^{-/-} HFD; one-way ANOVA) or UA (200 mg/kg; *right*) ($n = 3$; $P < 0.05$ for UA-treated NFD vs. UA-treated HFD, $^{\#}P < 0.05$ for UA-treated HFD vs. UA-treated TRPV₄EC^{-/-} HFD; one-way ANOVA).

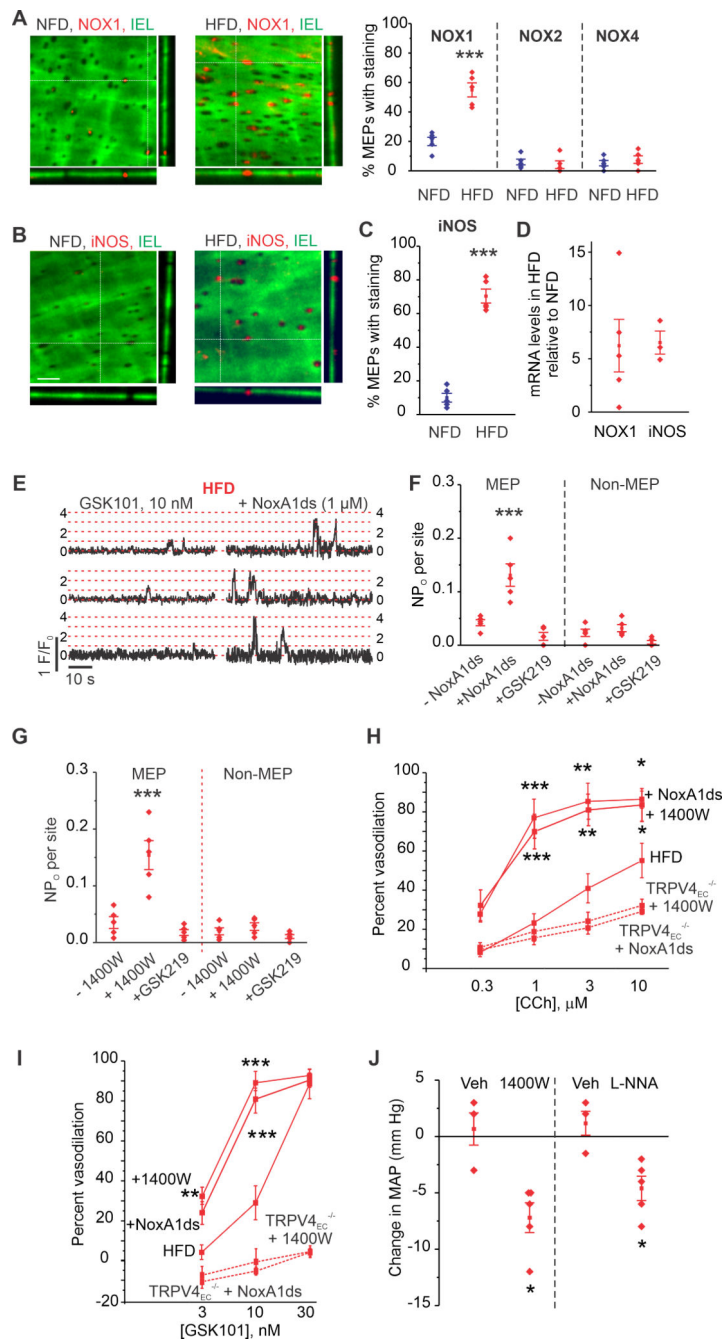


Figure 4. Localized NOX1 and iNOS upregulation underlies PN-induced impairment of TRPV4_{EC} channel activity in obesity.

(A) *Left*, representative merged z-stack images from *en face* preparations of third-order MAs showing IEL autofluorescence (green) and NOX1 immunofluorescence (red) in NFD (*left panel*) and HFD mice (*right panel*). *Right*, quantification of NOX1, NOX2, and NOX4 localization at MEPs in NFD and HFD mice (n = 5; ***P < 0.001 for NOX1 in HFD vs. NFD; one-way ANOVA). (B) Representative merged z-stack images of iNOS staining, scale: 10 μm. (C) Quantification of iNOS localization at MEPs in NFD and HFD mice (n = 5; P < 0.001 for iNOS in HFD vs. NFD, t-test). (D) Relative NOX1 and iNOS mRNA levels in

homogenates of whole MAs from HFD mice expressed relative to those from NFD mice (** $P < 0.01$ vs. NFD, one-way ANOVA, $n = 4-5$). (E) Representative F/F₀ traces showing the effect of the NOX1 inhibitor peptide NoxA1ds (1 μM) on TRPV4_{EC} sparklet activity (GSK101, 10 nM) in MAs from HFD mice. Dotted red lines indicate quantal levels. (F) Effects of NoxA1ds or negative control peptide (-NoxA1ds) on TRPV4_{EC} sparklet activity at MEP and non-MEP sites in fluo-4-loaded MAs from HFD mice ($n = 5$; $P < 0.001$ for sparklet activity at MEP sites in the presence vs. absence of NoxA1ds; one-way ANOVA). (G) TRPV4_{EC} sparklet activity (GSK101, 10 nM) at MEP sites in MAs from NFD and HFD mice in the absence or presence of the iNOS inhibitor 1400W (1 μM , $n = 5$; $P < 0.001$ for sparklet activity at MEP sites in the presence vs. absence of 1400W; one-way ANOVA). (H) Effects of NoxA1ds or 1400W on CCh (0.3–10 μM)-induced dilation of MAs from HFD, TRPV4_{EC}^{-/-} HFD, or AKAP150_{EC}^{-/-} HFD mice ($n = 5-8$; * $P < 0.05$; < 0.01 ; < 0.001 vs. HFD only; two-way ANOVA). (I) Effects of NoxA1ds or 1400W on GSK101 (3–10 nM)-induced dilation of MAs from HFD, TRPV4_{EC}^{-/-} HFD, or AKAP150_{EC}^{-/-} HFD mice ($n = 5-9$; $P < 0.05$; < 0.01 ; < 0.001 vs. HFD only; two-way ANOVA). (J) Change in mean arterial pressure (MAP) following i.p. injection of 1400W (10 mg/kg) or L-NNA (100 mg/kg) compared to HFD mice treated with vehicle (Veh, saline; $n = 3-5$; $P < 0.05$ for 1400W-treated HFD vs. Vehicle-treated [Veh, saline] HFD, $P < 0.05$ for L-NNA-treated HFD vs. Vehicle-treated HFD; t-test).

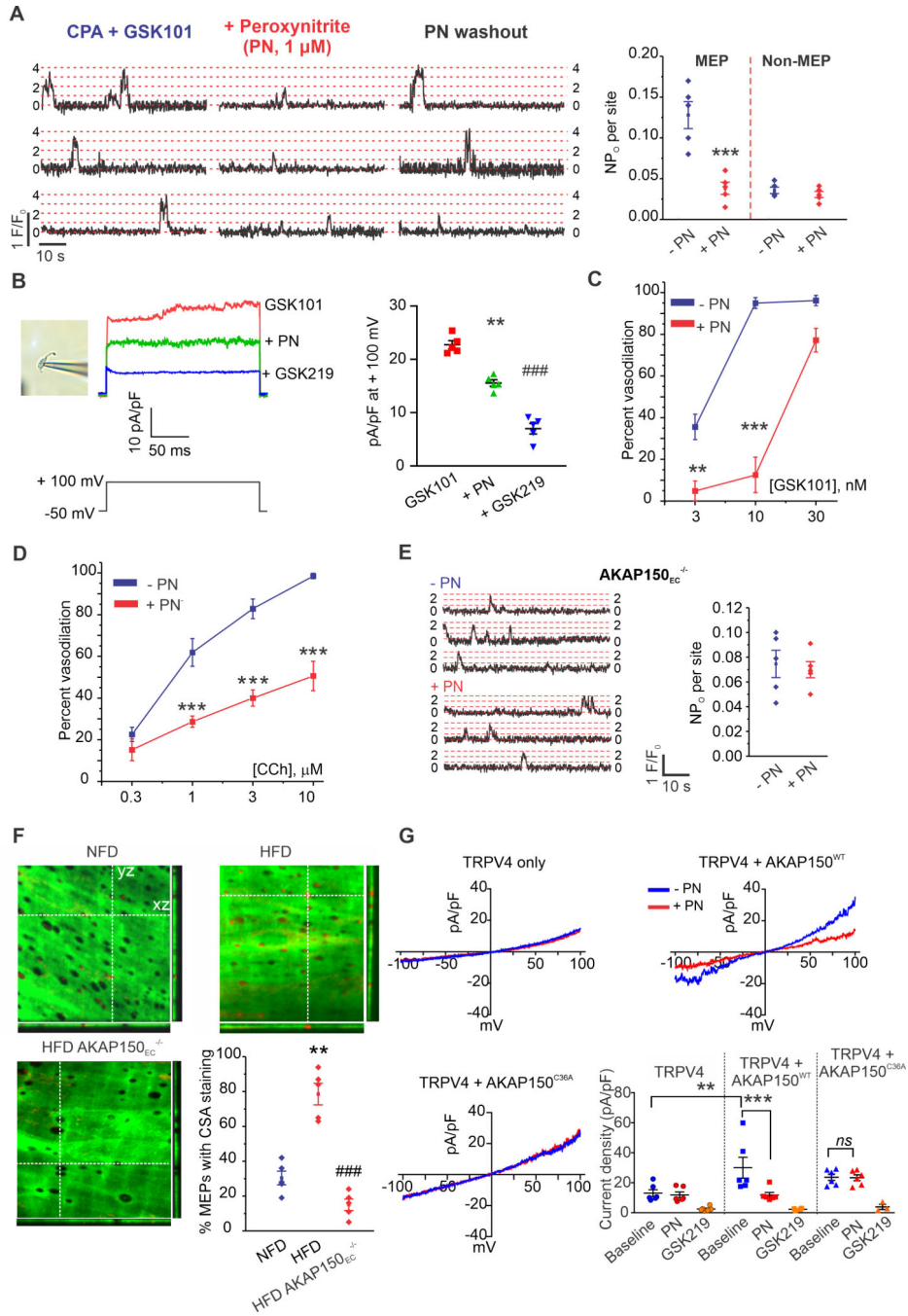


Figure 5. Peroxynitrite (PN) causes cysteine oxidation of AKAP150_{EC} to inhibit AKAP150_{EC}-PKC-TRPV4_{EC} signaling.

(A) Representative traces (*left*) and TRPV4_{EC} sparklet activity (NP_O) per site (*right*) indicating the effect of PN (1 μM) on TRPV4_{EC} sparklets at MEP and non-MEP sites in Fluo-4-loaded MAs from WT mice in the presence of CPA and GSK101 (10 nM). Dotted red lines indicate quantal levels. Data are presented as means ± SEM (n = 5; ***P < 0.001 for NP_O at MEP sites in the presence vs. absence of PN; one-way ANOVA). (B) *Left*, an image of EC in perforated patch configuration, *middle*, representative GSK101 (10 nM)-induced outward TRPV4_{EC} currents in freshly isolated ECs from WT mice and the effect of

PN (5 μM) and GSK219 (100 nM), a single pulse from a holding potential of -50 mV to $+100$ mV was applied in the presence of ruthenium red (1 μM) to inhibit Ca^{2+} -induced IK/SK currents, *right*, scatter plot showing TRPV4_{EC} currents in the presence of GSK101 alone, GSK101 + PN, and GSK101 + PN + GSK219 (n=5, ** $P < 0.01$ for GSK101 vs. PN; ### $P < 0.001$ for GSK101 vs. GSK219, one-way ANOVA). (C) Percent dilation in response to GSK101 (3–30 nM) in MAs from WT mice in the absence or presence of PN (n = 5–8; $P < 0.01$ [3 nM GSK101] and < 0.001 [10 nM GSK101] for percent dilation in the presence vs. absence of PN; two-way ANOVA). (D) Percent dilation of MAs from WT mice in response to CCh (0.3–10 μM) in the absence or presence of PN (n = 5–8; $P < 0.001$ [1 μM , 3 μM , and 10 μM CCh] in the presence vs. absence of PN; two-way ANOVA). (E) Representative F/F₀ traces (*left*) and scatter plot of TRPV4_{EC} sparklet activity (*right*, CPA + GSK101, 10 nM) in Fluo-4–loaded MAs from AKAP150_{EC}^{-/-} mice in the absence or presence of PN (1 μM , n = 5). (F) Representative merged images from *en face* preparations of third-order MAs showing IEL autofluorescence (green) and cysteine sulfenic acid (CSA) immunofluorescence (red) in NFD (*top-left*), HFD (*top-right*), and AKAP150_{EC}^{-/-} HFD (*bottom-left*) mice; quantification of CSA localization at MEPs (*bottom-right*) in NFD, HFD, and AKAP150_{EC}^{-/-} HFD mice (n=3; $P < 0.01$ for HFD vs. NFD; $P < 0.001$ for AKAP150_{EC}^{-/-} HFD vs. HFD; one-way ANOVA). (G) Representative current traces of GSK219-sensitive TRPV4 currents in HEK293 cells transfected with TRPV4 only (*top-left*), TRPV4+AKAP150^{WT} (*top-right*), and TRPV4+AKAP150^{C36A} (*bottom-left*) recorded in the whole-cell patch-clamp configuration. Current density plot (*bottom-right*) of GSK219-sensitive TRPV4 currents (n = 6; $P < 0.01$ for TRPV4 baseline vs. TRPV4+AKAP150^{WT} baseline, $P < 0.001$ for TRPV4+AKAP150^{WT} baseline vs. TRPV4+AKAP150^{WT} with PN; *ns* for TRPV4+AKAP150^{C36A} baseline vs. TRPV4+AKAP150^{C36A} with PN; one-way ANOVA).

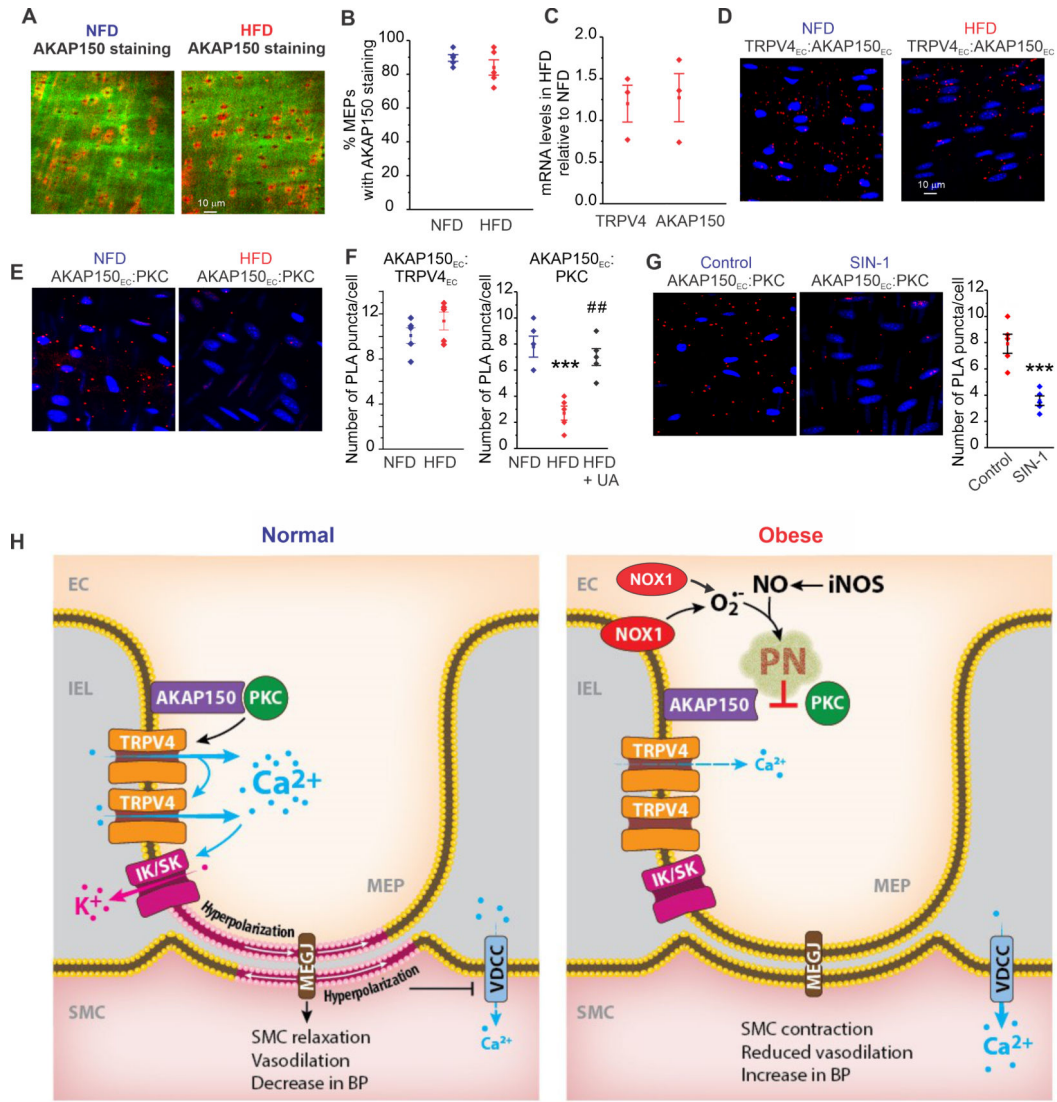


Figure 6. Peroxynitrite (PN) impairs AKAP150_{EC} anchoring of PKC in obesity.

(A) Representative merged images from *en face* preparations of third-order MAs showing IEL autofluorescence (green) and AKAP150_{EC} immunofluorescence (red) in NFD (*left*) and HFD mice (*right*). (B) Quantification of AKAP150_{EC} staining at MEPs in NFD and HFD mice (n = 5). (C) Quantification of TRPV4 and AKAP150 mRNA levels in homogenates of third-order MAs from HFD mice, expressed relative to those in NFD mice (n = 3). (D) Representative PLA merged images of EC nuclei (*blue*) and AKAP150_{EC}:TRPV4_{EC} co-localization (red puncta) in *en face* preparations of third-order MAs from NFD (*left*) and HFD (*right*) mice. (E) Representative PLA merged images of EC nuclei (*blue*) and AKAP150_{EC}:PKC co-localization (red puncta) in third-order *en face* preparations of MAs from NFD (*left*) and HFD (*right*) mice. (F) Quantification of AKAP150_{EC}:TRPV4_{EC} co-localization (*left*) and AKAP150_{EC}:PKC co-localization (*right*) in NFD and HFD mice. AKAP150_{EC}:PKC co-localization was rescued by uric acid (UA, 200 μM) in HFD mice (n = 5; ****P* < 0.001 for HFD only vs. NFD only, #*P* < 0.01 for UA-treated HFD vs. HFD only;

one-way ANOVA). (G) *Left*, representative PLA merged images of EC nuclei (*blue*) and AKAP150_{EC}:PKC co-localization (red) in MAs from WT mice in the absence or presence of 50 μ M SIN-1. *Right*, quantification of AKAP150_{EC}:PKC co-localization (*right*) in WT mice in the absence or presence of SIN-1 (n = 5; $P < 0.001$ vs. Control; t-test). (H) Schematic depicting the PN-dependent signaling mechanism that impairs endothelial function and elevates blood pressure in obesity.

Author Manuscript

Author Manuscript

Author Manuscript

Author Manuscript